Weighing Supported Nanoparticles: Size-Selected Clusters as Mass Standards in Nanometrology

N. P. Young, Z. Y. Li,* Y. Chen, S. Palomba, M. Di Vece, and R. E. Palmer

Nanoscale Physics Research Laboratory, School of Physics and Astronomy, University of Birmingham, Edgbaston, Birmingham B15 2TT, United Kingdom

(Received 2 April 2008; revised manuscript received 5 November 2008; published 9 December 2008)

We present a new approach to quantify the mass and 3D shape of nanoparticles on supports, using size-selected nanoclusters as mass standards in scanning transmission electron microscope. Through quantitative image intensity analysis, we show that the integrated high angle annular dark field intensities of size-selected gold clusters soft-landed on graphite display a monotonic dependence on the cluster size as far as ~6500 atoms. We applied this mass standard to study gold nanoparticles prepared by thermal vapor deposition and by colloidal wet chemistry, and from which we deduced the shapes of these two types of nanoparticles as expected.

DOI: 10.1103/PhysRevLett.101.246103 PACS numbers: 81.07.−b, 61.46.Bc, 61.46.Df, 68.37.Ma

Since the properties of nanoclusters and nanoparticles depend critically on their size [1,2], the measurement of their mass is crucial. For example, knowledge of the mass, i.e., the number of atoms in the clusters, when coupled with the measured projected area of the nanoparticles, would enable us to deduce the 3D shape of the nanoparticles. This is of particular importance in areas such as environmental health [3] and catalysis [4,5], because it regulates the effective surface area of the (typically supported) particles. However, atom counting is a challenging task for nanoparticles on surfaces, in terms of accuracy, efficiency, and mass range. Here we show that soft-landed size-selected atomic clusters can be used as mass standards which enable surface mass spectrometry by scanning transmission electron microscopy (STEM). For Au clusters on carbon surfaces, we find that the measured relationship between mass and the high angle annular dark field (HAADF) intensity in STEM displays a monotonic dependence on cluster size as far as ~6,500 atoms. This extends the applicable mass range for STEM-based mass spectrometry by about 3 orders of magnitude [6,7]. The method is demonstrated by the 3D shape determination of colloidal, evaporated and size-selected Au nanoparticles.

There are a number of ways that the masses of nanoparticles on surfaces can be measured. Cantilever-based techniques have recently been demonstrated for mass detection at the zeptogram level (10^{-21} g) [8,9]. Electron-microscopy-based techniques have a long history [6,7,10–18]. In Zeitler and Bahr's early work of 1962, the mass of nanoparticles has been determined down to 10^{-18} g using STEM with an accuracy of 10% [17]. The advantage of this approach is that the mass information obtained can be directly correlated to the structure and properties of the particle studied. The concept of *atomic-level* mass determination by STEM, as developed by Howie, is a quantitative application of the HAADF-STEM imaging method [18,19]. This requires an accurate knowledge of the electron scattering cross section (Ω) as a function of the number of atoms (N) and the number of electrons in the focused electron beam. *Ab initio* calculation of high angle electron scattering cross section of nanoparticles is a challenging task as factors such as multiple electron scattering, thermal diffuse scattering, and partial coherence of the focused electron probe have to be taken into account, and their absolute quantification is still a source of much theoretical debate [20]. Assuming a linear relationship between Ω and N, both the number of atoms in a cluster (to within ± 2 atoms) and the overall (oblate) shape were deduced for small clusters of 24 atoms [6,7]. We recently demonstrated experimentally that such linearity extends to much large sizes [21]. However, the experimental determination of the *absolute* cross section is still extremely challenging, as electron detectors of high dynamical range are required [6,22]. This has prevented the application of the STEM-based technique to a wide range of particle sizes, as one would wish. However, mass information can be obtained through STEM-based mass measurements if a known mass standard can be established. In biological applications, molecules of known molecular weight, such as ferritin, has been used as a mass standard for comparative measurements [12]. In materials science applications, a suitable standard for nanoparticle mass determination has so far been lacking.

Our approach is to use size-selected atomic clusters on supports as a mass standard to establish experimentally the relationship between atomic scattering cross section and the number of atoms. This builds upon our recent progress in atomic cluster beam technology [23–25], where a novel mass-selection technique based on the time-of-flight principle has been implemented into a radio frequency magnetron sputtering and gas aggregation cluster beam source. The source allows us to size-select positively charged particles from single atoms to the ~10 nm regime with a mass resolution of $M/\Delta M \approx 25$ which is independent of mass. In this study, we use Au as the target material and graphite as the substrate [26]. The kinetic energy of the clusters is chosen to be 500 eV, to prevent fragmentation of the clusters upon landing [27,28].

Figures 1(a)–1(c) show three representative HAADF-STEM images of clusters with selected mass size of 147, 2057, and 6525 atoms, respectively. The STEM images were obtained using an FEI Tecnai F20 electron microscope with a field emission gun at an accelerating voltage of 200 kV. A Fischione 3000 HAADF detector was used to record images at an inner collection angle of 50 mrad and outer collection angle of 150 mrad, with an incident probe size of around 4 Å. The gain and offset of the amplifier were set in such a way that the detector was working far below its saturation level, while at the same time single atom sensitivity could still be achieved (as verified by post-acquisition image analysis). Every effort was made to keep the imaging conditions constant, particularly the emission current. The emission current was stable throughout each experimental run to within 1 μA. The same specimen, with Au_{309} clusters, was used as a check between different runs. It was found that the change in integrated intensity induced by emission current was smaller than the statistical errors. In the images, atomic columns were not resolved within the clusters, yet single atoms were sometimes detected on the substrate, mostly in the vicinity of the deposited clusters. No rafts of Au atoms were detected. This has been confirmed by further observations using aberration-corrected STEM where single atom detection is more straightforward. Figure 1(d) displays the HAADF intensity integrated over the clusters as a function of the number of atoms within the clusters. The image intensity analysis is performed using SPIP software (version 3.2.0.1, Image Metrology). Integrated STEM intensities were obtained after background subtraction. The choice of size over which the integrated intensity obtained varied with the size of the particles. This is to ensure that all atoms, including those single atoms at the vicinity of the particles, are accounted for in the quantitative intensity analysis. The intensity is taken from the mean value of the distribution while the standard deviation is used for estimating of the error bars. It can be seen that initially the intensity increases rapidly with the number of atoms, and then the rate slows down. A log-log fit (inset) shows that the data fit well to the relationship, $I = 68\,852N^{0.92315}$, with a fitting residual of $R = 0.997\,33$. This monotonic relation offers a calibration of the *true* mass of the nanoparticles. Although the size selection of the clusters has been studied up to 30 000 atoms, quantitative intensity analysis has only been performed for N up to 6500. This is due to that the source of the error bars in Fig. 1(d) includes not only microscope stability, substrate uniformity, thickness, and local structure, but also strong dynamical scattering in large nanoparticles. The latter results in the increased uncertainty with the size of clusters. $N \sim 6500$ can thus be viewed as the upper limit of this method.

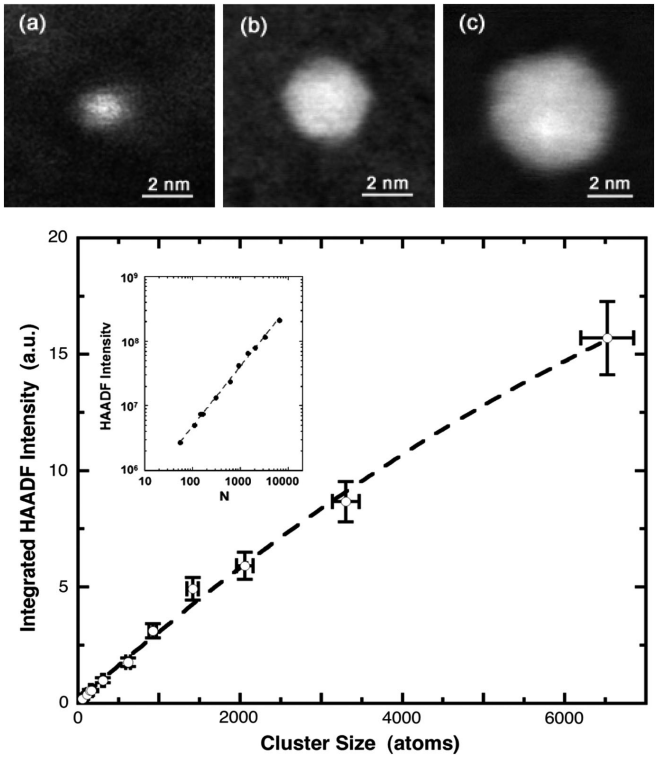

FIG. 1. HAADF-STEM images and their intensity analysis. (a)–(c) Representative images of Au clusters with selected mass of 147, 2057, and 6525 atoms on graphite supports. The images were obtained at 900 kX magnification at a resolution of 1024×1024 pixels and they were low-pass filtered. (d) The HAADF intensity integrated over clusters as a function of number (N) of Au atoms in the clusters. The error bars were taken from the standard deviation of distribution measured by STEM. The inset shows the logarithmic fit of the intensity versus N, $I = 68\,862N^{0.92315}$. The residual of the fit $R = 0.99733$.

We applied the calibration curve in Fig. 1(d) to study Au nanoparticles prepared via two different approaches. In the first case, colloidal Au particles, obtained from Agar Scientific, were drop cast on to a TEM grid coated with an amorphous carbon film. In the second case, the sample was deposited on an amorphous carbon thin film in a vacuum of 10^{-7} mbar through thermal sublimation of 99.99% purity Au. Representative HAADF-STEM images for the two types of nanoparticles are shown in Figs. 2(a) and 2(b), respectively. Most of particles are circular in two-dimensional (2D) projection, except for a few closely spaced clusters that seem to be touching. The histograms of the diameters in 2D projection of both types of nanoparticles are shown in (c) and (d). The difference in the diameter distributions shown can be related to the ways that the particles were formed. During the wet chemical preparation of the gold colloids, a reasonable degree of size-selection has been achieved by carefully controlling the reaction time, yielding particles with an average diameter of 5 nm, as specified by the supplier. In the case of vapor deposited Au atoms, the size distribution is much broader as the cluster nucleation depends on Au adatom diffusion as well as the density of surface defects.

The above conventional analysis only provides size information in 2D projection, where the depth information along the electron beam direction is missing. In the case of the HAADF-STEM imaging mode this information is in-

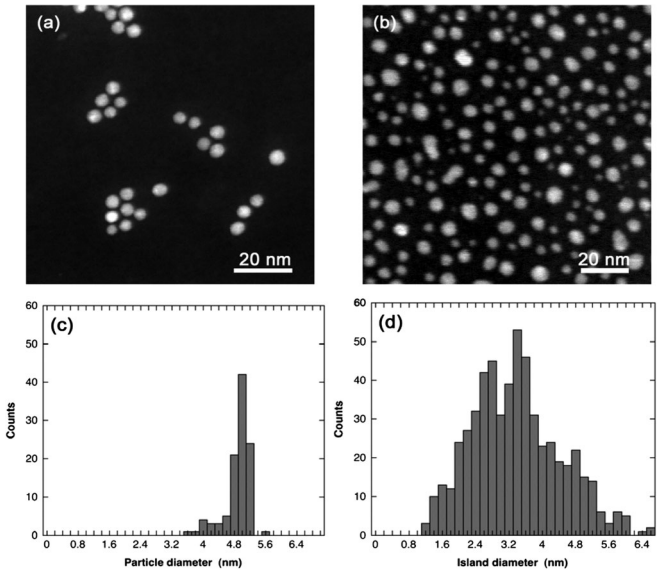

FIG. 2. HAADF-STEM images taken from Au nanoparticles deposited on a Cu TEM grid coated with amorphous carbon thin film. (a) The nanoparticles were prepared by wet chemistry method. (b) The nanoparticles were prepared by thermally evaporating Au onto the TEM grid held at room temperature under high vacuum condition. The corresponding size distribution is shown in (c) and (d), respectively.

cluded in the image intensity. Using the I-N relationship shown in Fig. 1(d), we calibrate the number of Au atoms (N) in both types of nanoparticles against those in the size-selected Au clusters. The results allow us to plot, in Fig. 3, the 2D projection diameter D of the particles as a function of $N^{1/3}$. Those particles touching each other have been excluded from this analysis. The linear relationship between D and $N^{1/3}$ for all three samples implies that the shape of nanoparticles is three-dimensional rather than planar, as otherwise linearity should be found for D versus $N^{1/2}$. It is also most interesting to see the distinctive trends in the Au nanoparticle shapes formed by the different methods of preparation. The solid and dashed lines display the $D \sim N^{1/3}$ relations derived from a simple spherical geometric model, $D_s = \kappa N^{1/3}$, and from a hemispherical model, $D_h = \kappa(2N)^{1/3}$. Here, $\kappa = 0.41$ nm, representing the effective diameter of Au atoms, is obtained from fitting to the experimental data. This value is slightly larger than twice of the Wigner-Seitz radius, $R = 0.17$ nm, for Au [29]. It is the most striking that the data from the thermally evaporated Au nanoparticles are consistent with the hemispherical model, while the data from the colloidal Au nanoparticles agree with the spherical model, as one would expect. This latter result suggests that the organic ligands on the particles surface not only prevent aggregation of the nanoparticles in solution, but also help in maintaining their pseudospherical shapes even when they are dried on the substrate. For the size-selected Au clusters, preformed in the gas phase and deposited on the surface, the result implies that the soft-landing has successfully preserved

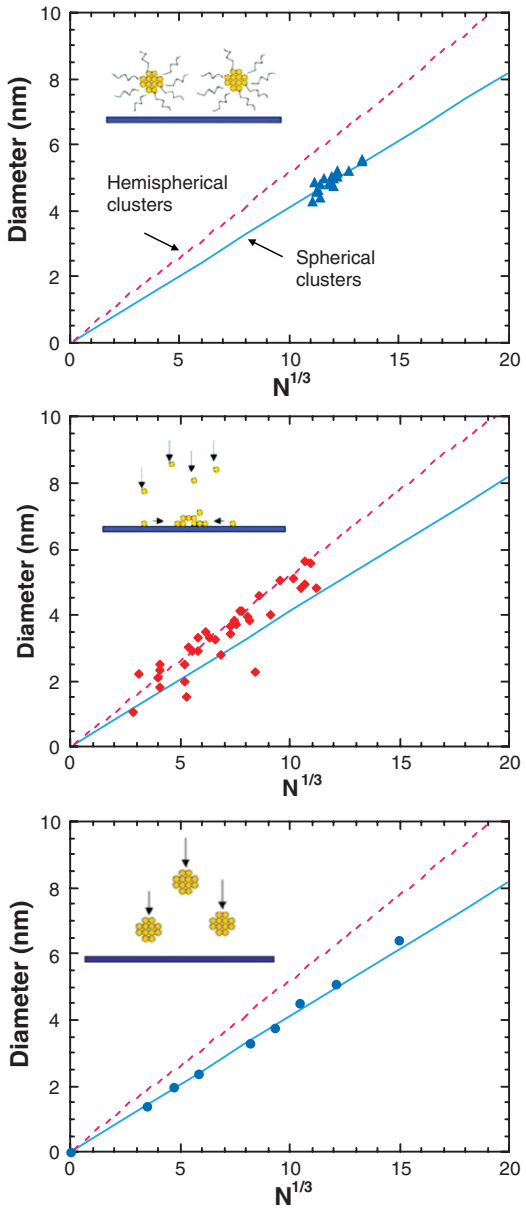

FIG. 3 (color). Relationship between particle diameter and $N^{1/3}$ for Au nanoparticles prepared by three different methods. (a) Colloidal nanoparticles, (b) nanoparticles by thermal evaporation, and (c) size-selected clusters preformed in gas phase and soft landed on the surface. Spherical cluster approximation (the blue solid line) and hemispherical cluster approximation (the red dashed line) are shown to allow comparison of overall particle geometry. Schematics of growth mechanism of Au nanoparticles are also shown in the insets.

the pseudospherical shape of the clusters on the surface. This also indicates that the graphite is a nonwetting support for Au particles at the nanoscale, which is consistent with the morphology of Au clusters found on amorphous carbon films using high resolution TEM [30].

The above two cases have demonstrated that the highly size-selected clusters provide an excellent mass standard. They allow us to obtain a *true* calibration curve for the par-

ticle mass-HAADF intensity relationship over a large mass range, thus allowing the full realization of the potential of the HAADF-STEM technique for surface mass spectrometry. Previously, all measurements have been based on the assumption of the linearity of the mass-intensity relationship. Here we demonstrate for the first time that the experimentally measured monotonic mass-intensity relationship allows extension of the applicable mass range for STEM-based mass spectrometry up to about 6500 atoms for Au, which is about 3 orders of magnitude wider than previously reported [6,7]. In addition, we are working on the soft landing of very small clusters so that the calibration curve can be extended towards the single atom level. The availability of such a wide range of size-selected clusters also provides a real possibility of independent determination of the electron scattering cross sections of nanoparticles [21], which is vital for physical understanding of the critical issues involved in electron scattering. In our approach, the mass resolution depends on the resolution of the mass selection of clusters. For the Birmingham cluster source, $M/\Delta M$ is $\sim$25 over the size range studied [23–25]. This can be readily improved to $\sim$100 or better with some modification of the existing system. The better stability, higher signal-to-noise ratio, and lower background offered by the new generation aberration-corrected electron microscope is expected to further reduce the statistical errors in HAADF intensity measurements.

For the characterization of the 3D morphology of nanoparticles, STEM electron tomography is a very powerful technique and has been successfully employed for embedded and stable nanoparticles [31]. The main limitation of the technique is the time required to take full tomographs. This excludes many electron beam sensitive samples from analysis. Our method employs a ''single-shot''-type approach to a three-dimensional measurement problem. Gold was used as a model system in the present study, but the principle should be applicable for nanoparticles of other compositions, such as the platinum group metals commonly used in catalysis, although the extension to light elements will depend on the ability of separating signals from particles and from the substrate. It is envisaged that HAADF-STEM-based mass spectrometry would be very useful in the metrology of nanoparticles where knowledge of the particle mass and structure is desirable. For example, industrial catalyst particles often have complex morphologies rather than commonly assumed near spherical shapes. The complexity of the structure at the atomic level would directly affect the performance of the catalyst [5]. Furthermore, direct comparison of the measurements against the size-selected clusters of a known structure will allow more realistic modeling of nanoparticles with complex structures, thus enhancing the power to predict the physical properties associated with the structures. The ease of transport of mass-selected clusters deposited on standard carbon coated TEM grids suggests that they are ideal calibration standards for sharing between different laboratories.

This work was supported by the U.K. Engineering and Physical Science Research Council (EPSRC).

*ziyouli@nprl.ph.bham.ac.uk

[1] P. Jena and A. W. Castleman, Proc. Natl. Acad. Sci. U.S.A. **103**, 10 560 (2006).
[2] H.-G. Boyen *et al.*, Science **297**, 1533 (2002).
[3] K. Wittmaack, Environ. Health Perspect. **115**, 187 (2007).
[4] M. D. Hughes, Nature (London) **437**, 1132 (2005).
[5] J. K. Norskov and C. H. Christensen, Science **312**, 1322 (2006).
[6] A. Singhal, J. C. Yang, and J. M. Gibson, Ultramicroscopy **67**, 191 (1997).
[7] J. C. Yang, S. Bradley, and J. M. Gibson, Mater. Charact. **51**, 101 (2003).
[8] Y. T. Yang, C. Callegari, X. L. Feng, K. L. Ekinci, and M. L. Roukes, Nano Lett. **6**, 583 (2006).
[9] M. Li, H. X. Tang, and M. L. Roukes, Nature Nanotech. **2**, 114 (2007).
[10] J. S. Wall and J. F. Hainfield, Annu. Rev. Biophys. Biophys. Chem. **15**, 355 (1986).
[11] S. A. Müller and A. Engel, Micro **32**, 21 (2001).
[12] B. Feja and U. Aebi, Micro **30**, 299 (1999).
[13] M. M. J. Treacy and S. B. Rice, J. Microsc. **156**, 211 (1989).
[14] A. Carlsson, A. Puig-Molina, and T. V. W. Janssens, J. Phys. Chem. B **110**, 5286 (2006).
[15] L. D. Menard, F. Xu, R. G. Nuzzo, and J. C. Yang, J. Catal. **243**, 64 (2006).
[16] L. D. Menard *et al.*, J. Phys. Chem. **110**, 12874 (2006).
[17] E. Zeitler and G. F. Bahr, J. Appl. Phys. **33**, 847 (1962).
[18] A. Howie, J. Microsc. **117**, 11 (1979).
[19] M. S. Isaacson, D. Kopf, M. Ohtsuki, and M. Utlaut, Ultramicroscopy **4**, 101 (1979).
[20] A. Howie, Ultramicroscopy **98**, 73 (2004).
[21] Z. Y. Li, N. P. Young, M. Di Vece, S. Palomba, R. E. Palmer, A. L. Bleloch, B. C. Curley, R. L. Johnston, J. Jiang, and J. Yuan, Nature (London) **451**, 46 (2008).
[22] J. M. LeBeau, S. D. Findlay, L. J. Allen, and S. Stemmer, Phys. Rev. Lett. **100**, 206101 (2008).
[23] I. M. Goldby, B. von Issendorff, L. Kuipers, and R. E. Palmer, Rev. Sci. Instrum. **68**, 3327 (1997).
[24] B. von Issendorff and R. E. Palmer, Rev. Sci. Instrum. **70**, 4497 (1999).
[25] S. Pratontep, S. J. Carroll, C. Xirouchaki, C. M. Streun, and R. E. Palmer, Rev. Sci. Instrum. **76**, 045103 (2005).
[26] We find that, as long as the film thickness (graphite flakes or amorphous carbon films) is comparable and the substrate is locally uniform around the deposited clusters, the integrated HAADF intensity from clusters with the same size is comparable from the two similar substrates.
[27] R. E. Palmer, S. Pratontep, and H.-G. Boyen, Nature Mater. **2**, 443 (2003).
[28] S. Pratontep, P. Preece, C. Xirouchaki, R. E. Palmer, C. F. Sanz-Navarro, S. D. Kenny, and R. Smith, Phys. Rev. Lett. **90**, 055503 (2003).
[29] B. M. Smirnov, *Clusters and Small Particles in Gases and Plasmas* (Springer, New York, 2000).
[30] B. Pauwels *et al.*, Phys. Rev. B **62**, 10 383 (2000).
[31] E. M. Vogel, Nature Nanotech. **2**, 25 (2007).